Research towards application of diamond and silicon as cryogenic BLMs for LHC magnets

Marcin Bartosik - CERN BE-BI-BL

Plan

1. Motivation
2. Radiation hardness tests of detectors in cryogenic temperatures
3. Tests of detectors in magnetic field

Motivation

LHC / HL-LHC Plan

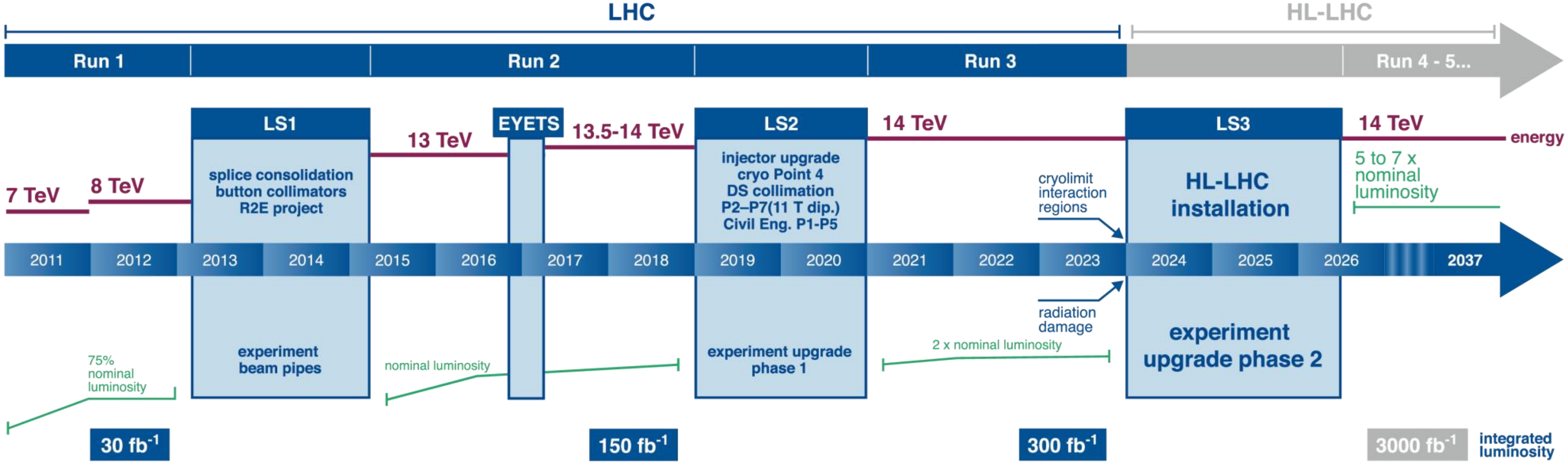

LHC/ HL-LHC Plan
(last update 22.02.2016)

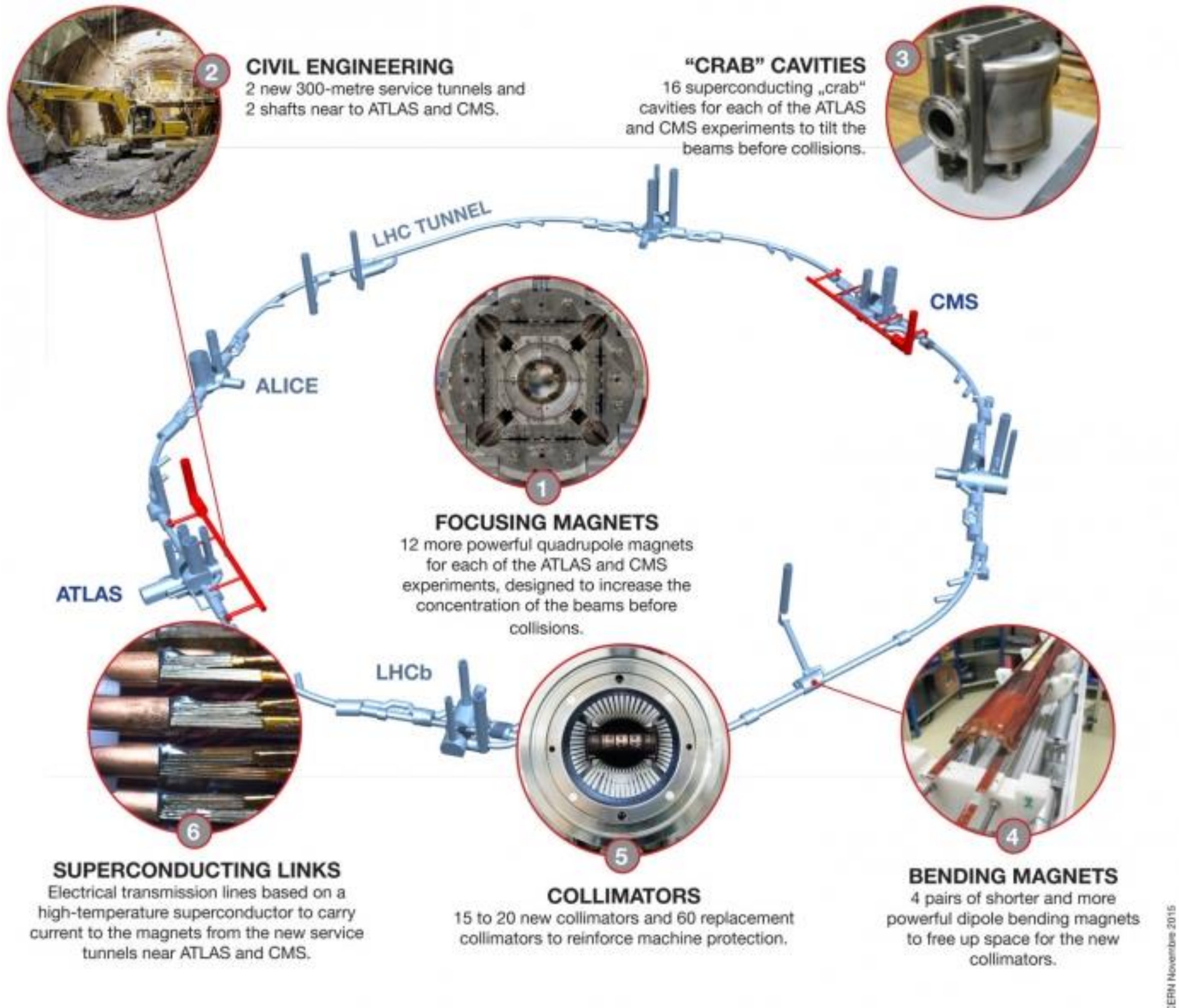
CIVIL ENGINEERING
2 new 300-metre service tunnels and 2 shafts near to ATLAS and CMS.
"CRAB" CAVITIES
16 superconducting „crab" cavities for each of the ATLAS and CMS experiments to tilt the beams before collisions.
LHC TUNNEL
CMS
ALICE
FOCUSING MAGNETS
12 more powerful quadrupole magnets for each of the ATLAS and CMS experiments, designed to increase the concentration of the beams before collisions.
ATLAS
LHCb
SUPERCONDUCTING LINKS
Electrical transmission lines based on a high-temperature superconductor to carry current to the magnets from the new service tunnels near ATLAS and CMS.
COLLIMATORS
15 to 20 new collimators and 60 replacement collimators to reinforce machine protection.
BENDING MAGNETS
4 pairs of shorter and more powerful dipole bending magnets to free up space for the new collimators.
CERN Novembre 2015

Cryogenic BLMs for HL-LHC

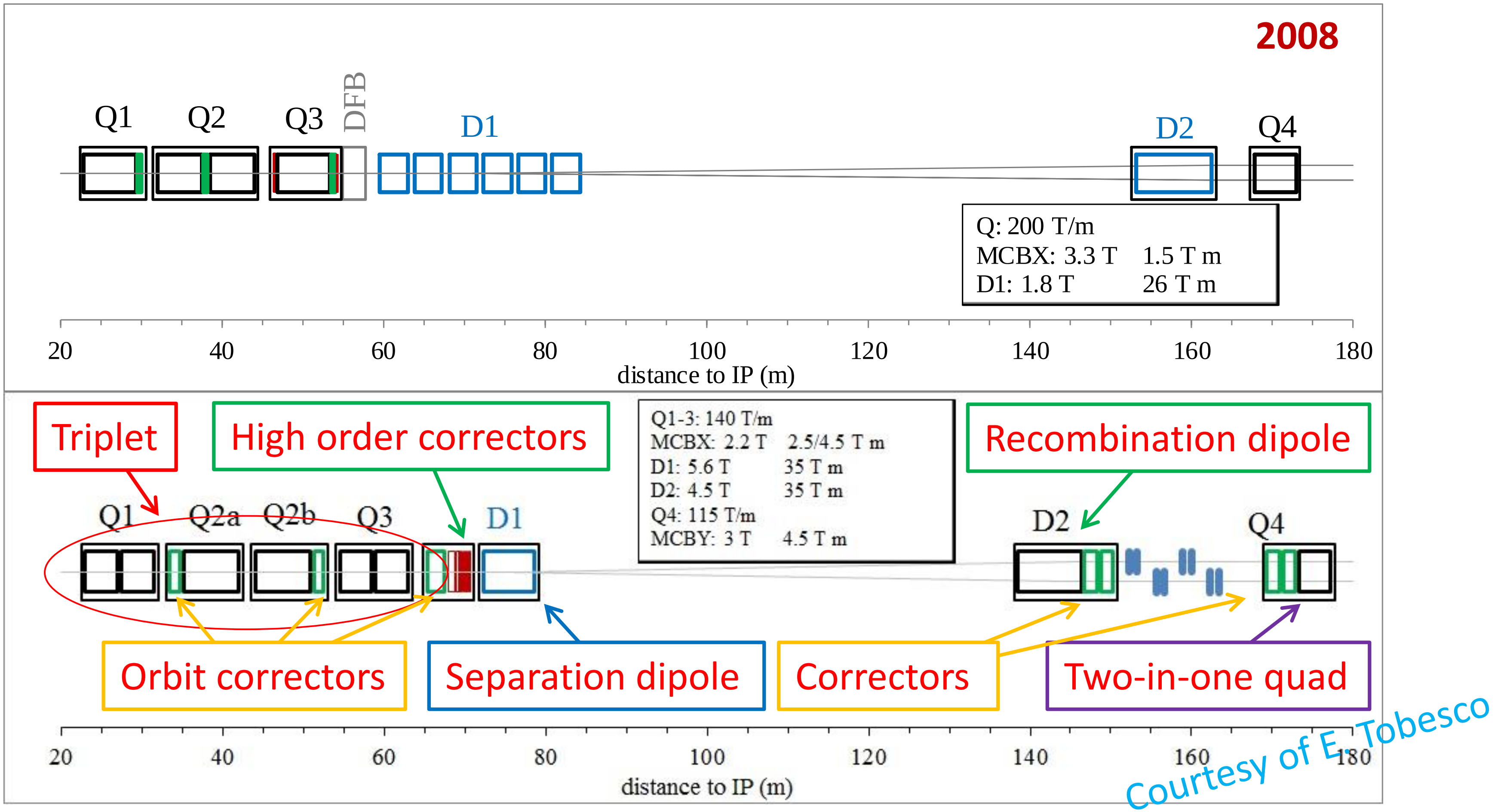

Cryogenic BLMs for HL-LHC

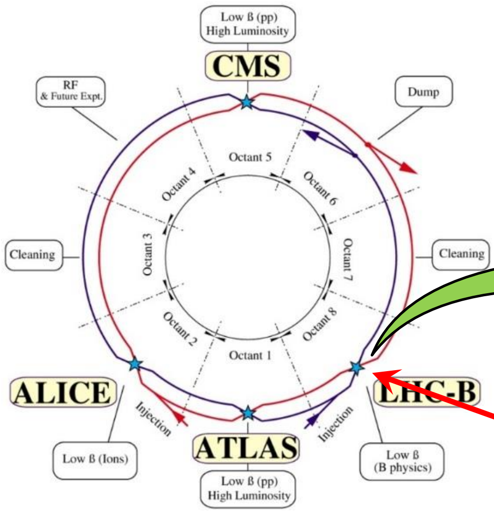

Overview of LHC ring with four main experiments

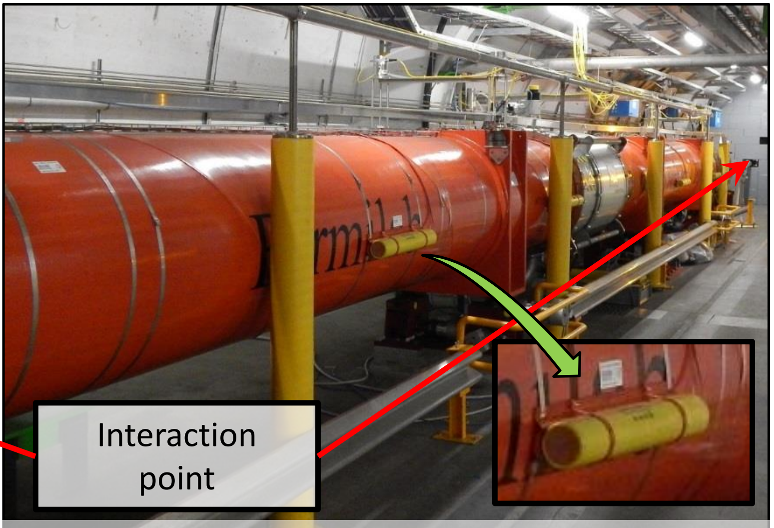

LHC triplet magnets left of LHC-b experiment

Requirements of Cryogenic BLMs

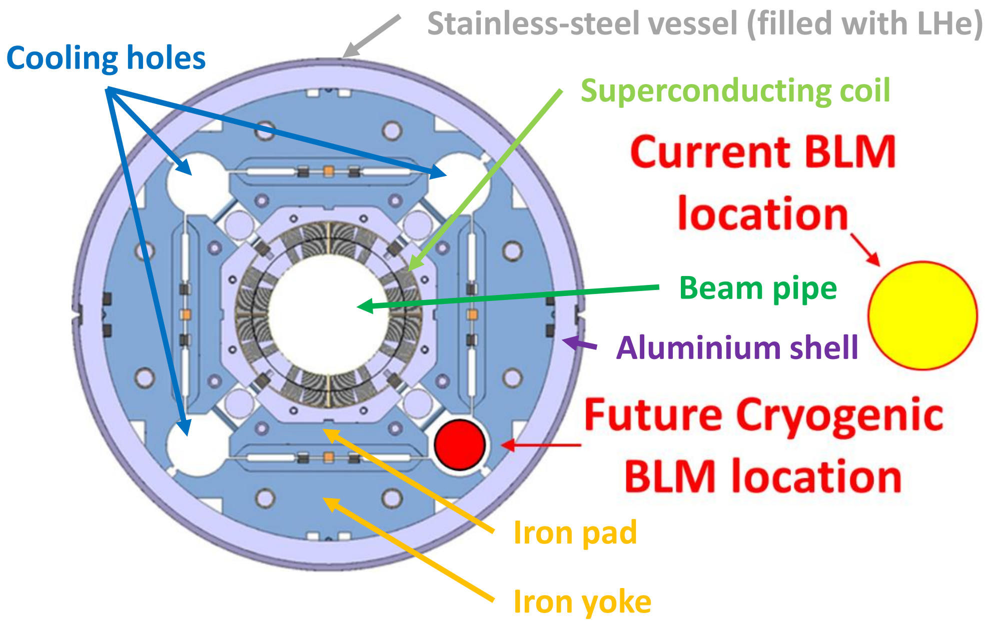

Inner Triplet Quadruples (MQXF) for HL-LHC (MQXFS1 Quadrupole design report)

Mechanical requirements:

- **total radiation dose of 2MGy,**
- **low temperature of 1.9K,**
- 20 years, maintenance free operation,
- resistance to magnetic field of 2T,
- resistance to a pressure of 1.1 bar, and capability of withstanding a fast pressure rise up to 20bar in case of a magnet quench.

Electronic requirements:

- direct current readout,
- response linear between 0.1 and 10 mGy/s, and
- response time faster than 100 µs.

Radiation hardness tests of detectors in cryogenic temperatures

Cryogenic irradiations

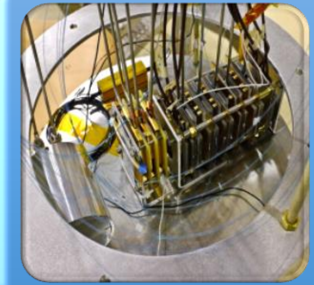

December 2012 (Superfluid helium environment of **1.9K**)

- 6 × p^+-n-n^+ silicon detectors, different intrinsic resistivity, 300µm thick, aluminium metalized.
- 2 × scCVD diamond detectors, 500µm thick, titanium and gold metalized.
- Integrated fluence of **1.225(85) · 10^{16} protons/cm^2**

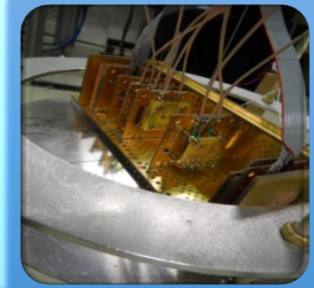

November 2014 (Liquid helium environment of **4.2K**)

- 2 × p^+-n-n^+ silicon detectors, same intrinsic resistivity of 10kΩcm, 300µm and 100µm thick.
- 2 × 3D detectors (silicon and scCVD diamond).
- Integrated fluence of **2.83(24) · 10^{15} protons/cm^2**

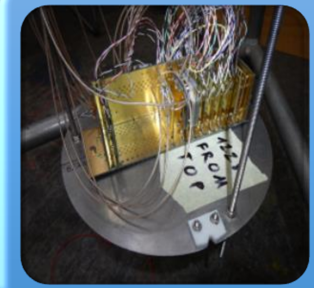

October 2015 (Liquid helium environment of **4.2K**)

- 18 × different p^+-n-n^+ silicon detectors, aluminium metallized.
- 2 × scCVD diamond detectors 300µm and 500µm thick, chromium and gold metalized.
- Integrated fluence of **6.84(48) · 10^{15} protons/cm^2**

Cryogenic apparatus

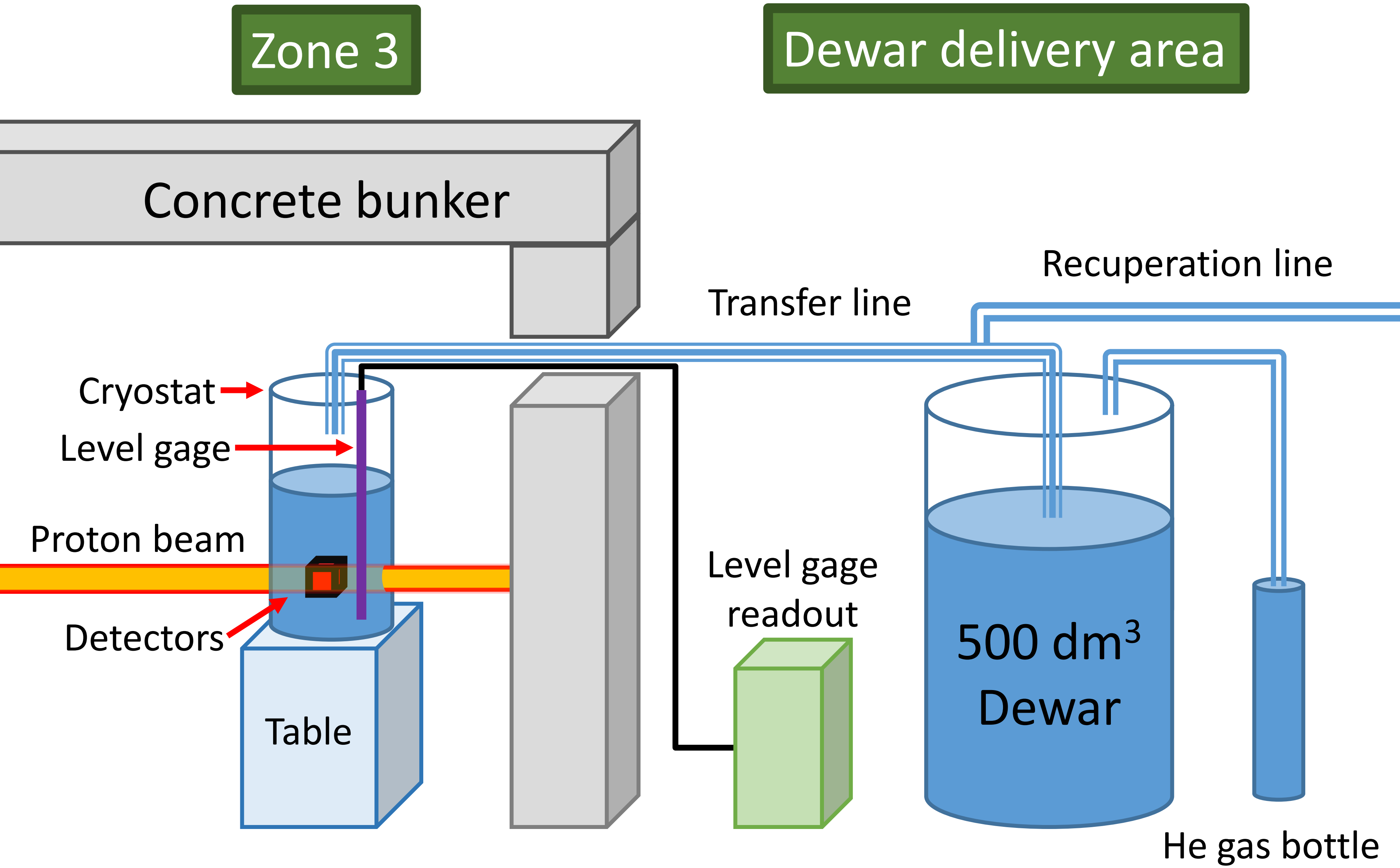

Cryogenic Irradiation – October 2015

- **2 × scCVD diamond detectors from Element Six (UK) Ltd. (300µm and 500µm thick), chromium and gold metalized at GSI by Mladen Kiš.**
- 18 × different p^+-n-n^+ silicon detectors, aluminium metallized.
- 2 × independent DC readout systems.
- Liquid helium environment of 4.2K.
- Total integrated fluence of **$6.84(48) \cdot 10^{15}$ protons/cm^2**,
  - Total dose of 1.82(13) MGy for silicon and 1.91(13) MGy for diamond,
  - Up to $1.1 \cdot 10^{11}$ protons/cm^2 per spill,
  - 24 GeV/c particle momentum.

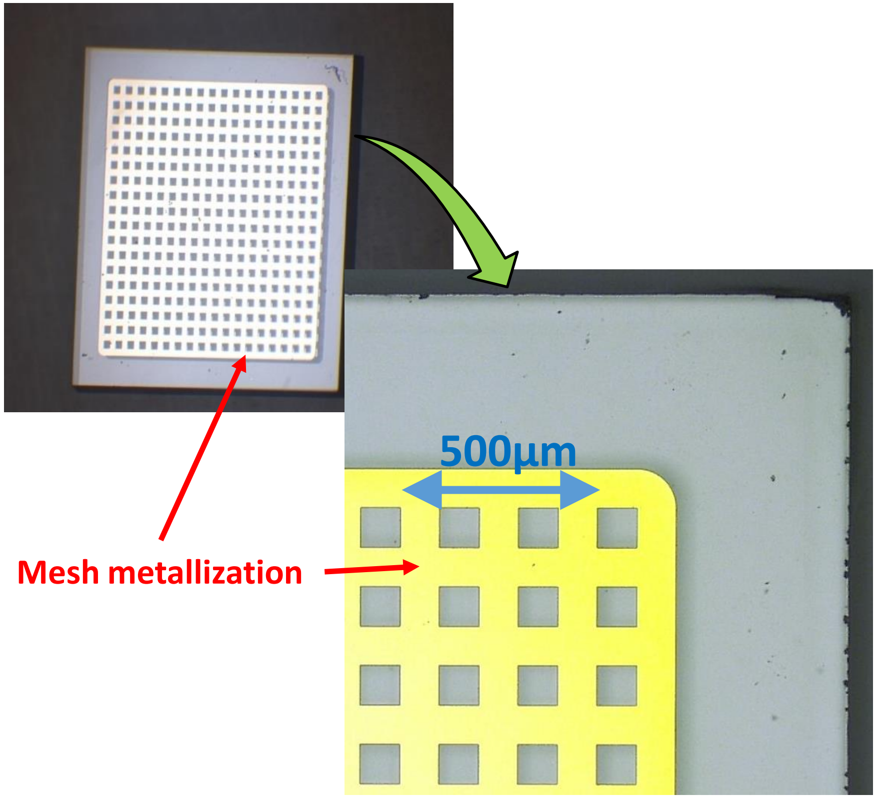

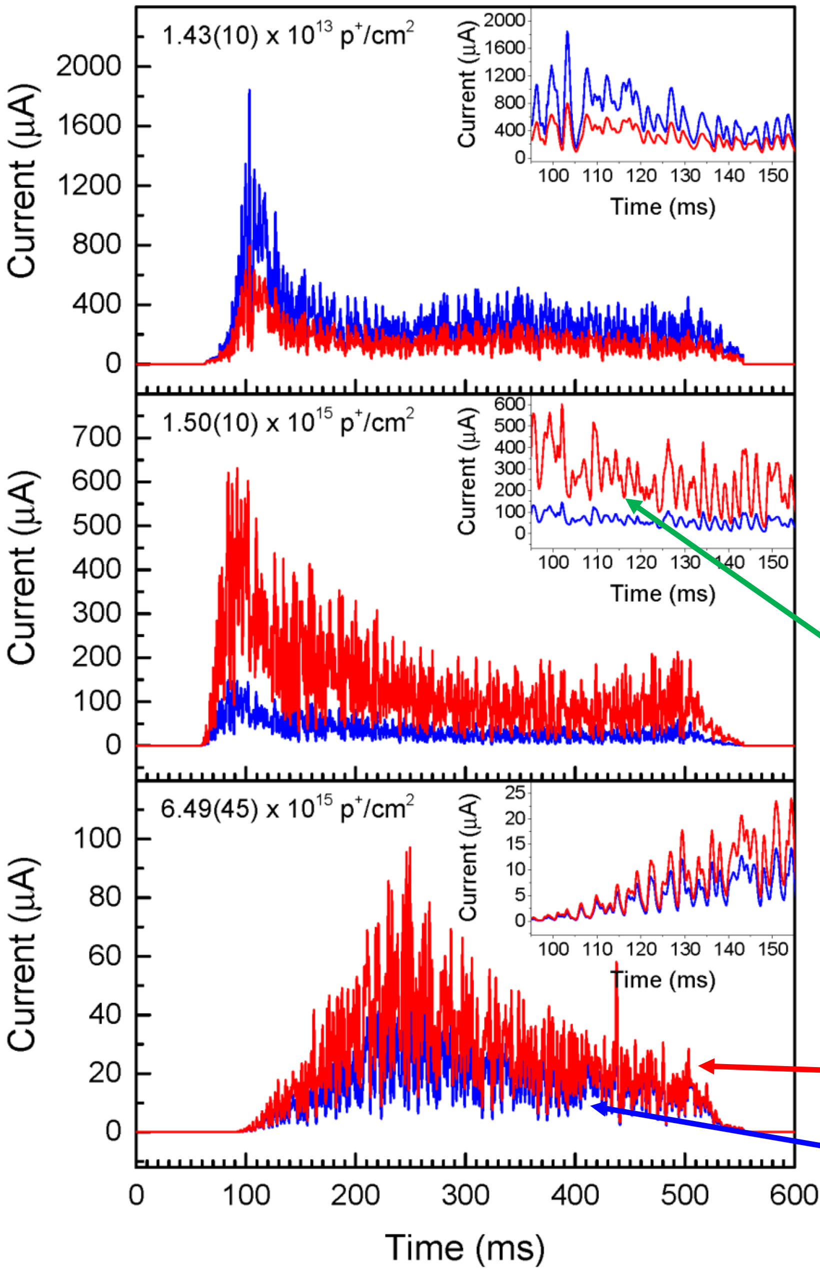

DAQ

- 120000 DC, spill induced, signals were recorded with 62.5nA current and 2μs time resolution.
- In the middle of the irradiation an additional DC components were observed when V_B on D1 and D2 was >100V (These signals were excluded from further analysis).

300μm CVD diamond

300μm n^+-n-p^+ Si

Results – charge vs. fluence

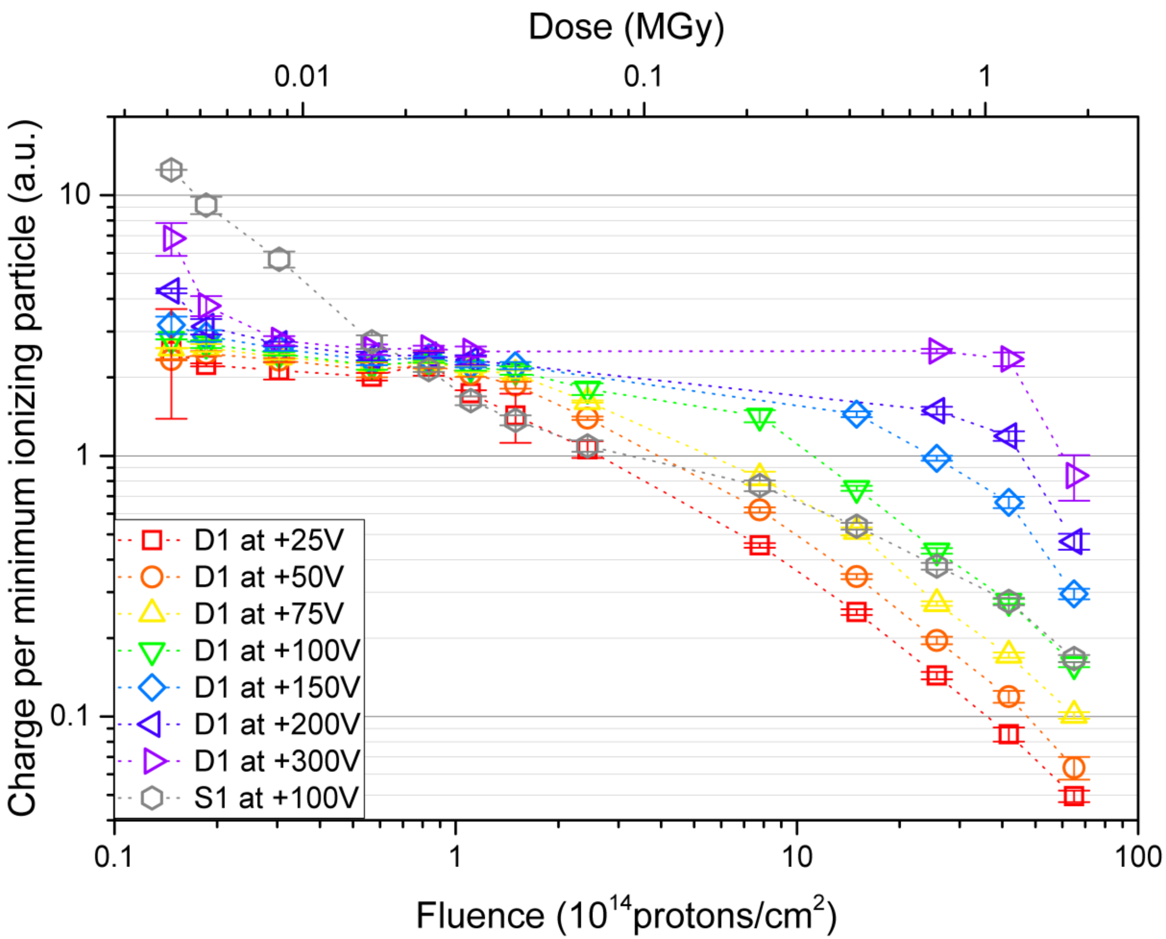

- D1 - 300µm thick scCVD diamond detector.
- S1 - 300µm thick p^+-n-n^+ Si detector added for a comparison.
- During the irradiation $Q/MIP_{D1}(+300V)$ decreased factor 8.1(28).

Results – charge vs. fluence

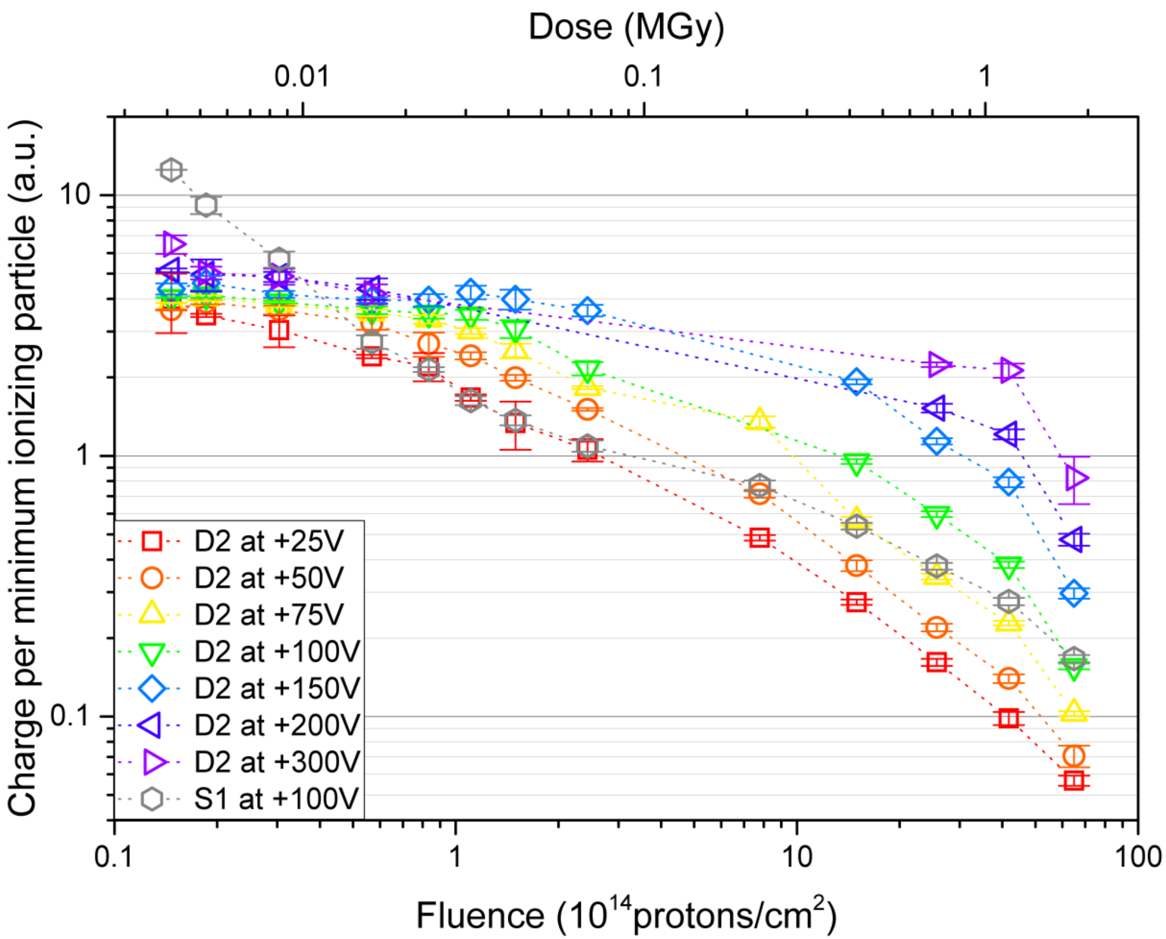

- D2 - 500µm thick scCVD diamond detector.
- S1 - 300µm thick p^+-n-n^+ Si detector added for a comparison.
- During the irradiation Q/MIP_{D2}(+300V) decreased factor 7.9(23).

Results – charge vs. fluence

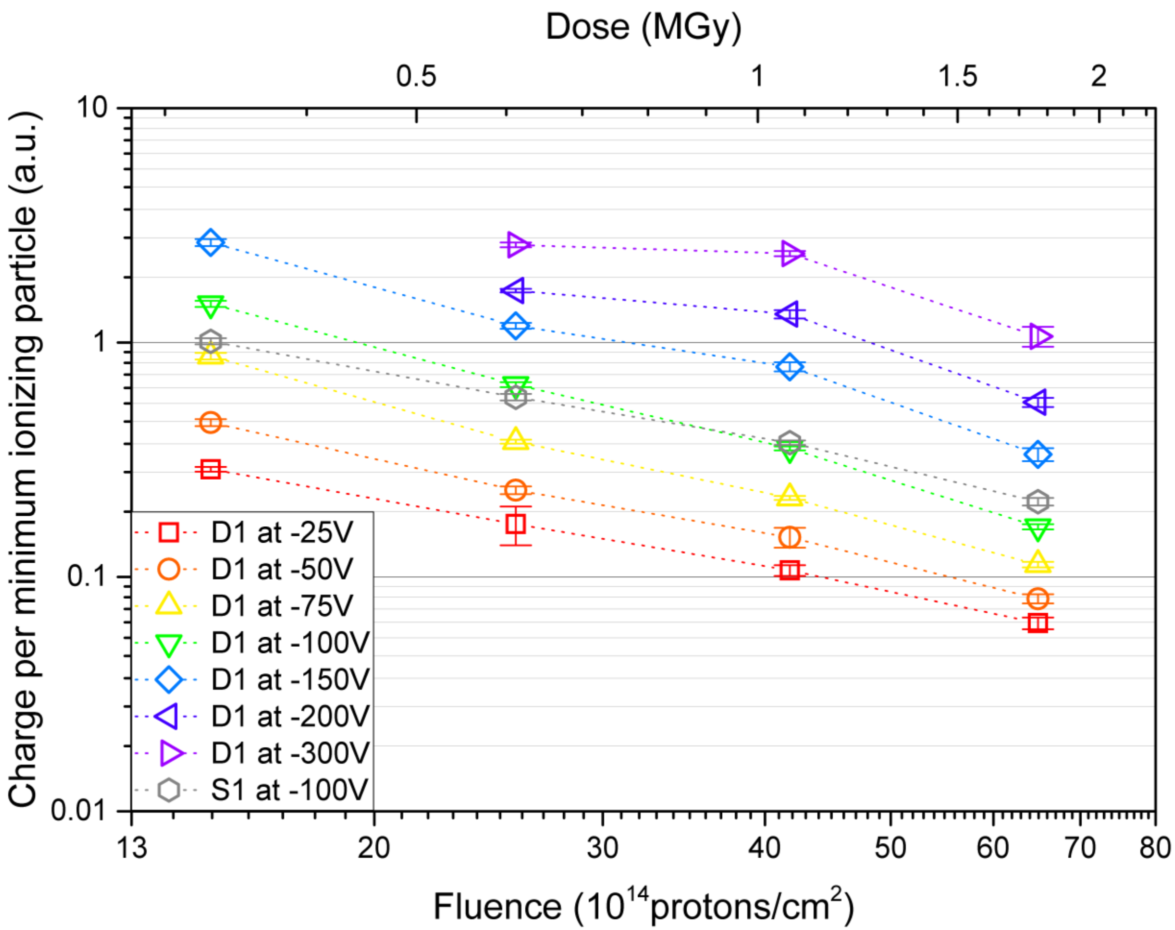

- All detectors biased by the same voltage.
- After reaching F=1.50(10)×10^{15} protons/cm^2 was possible to apply forward bias on Si detectors.

Results – charge vs. fluence

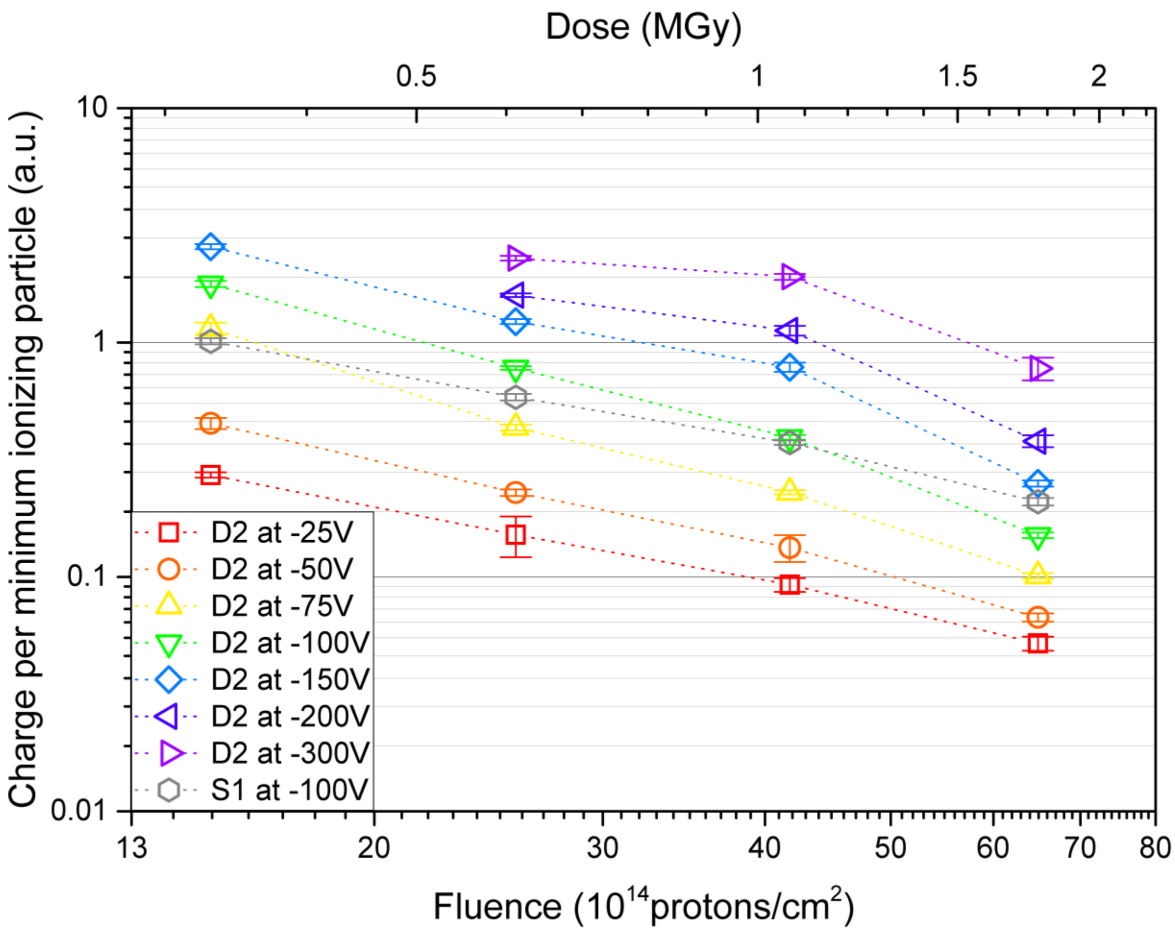

- All detectors biased by the same voltage.
- After reaching F=1.50(10)×10^{15} protons/cm^2 was possible to apply forward bias on Si detectors.

Results – charge vs. fluence

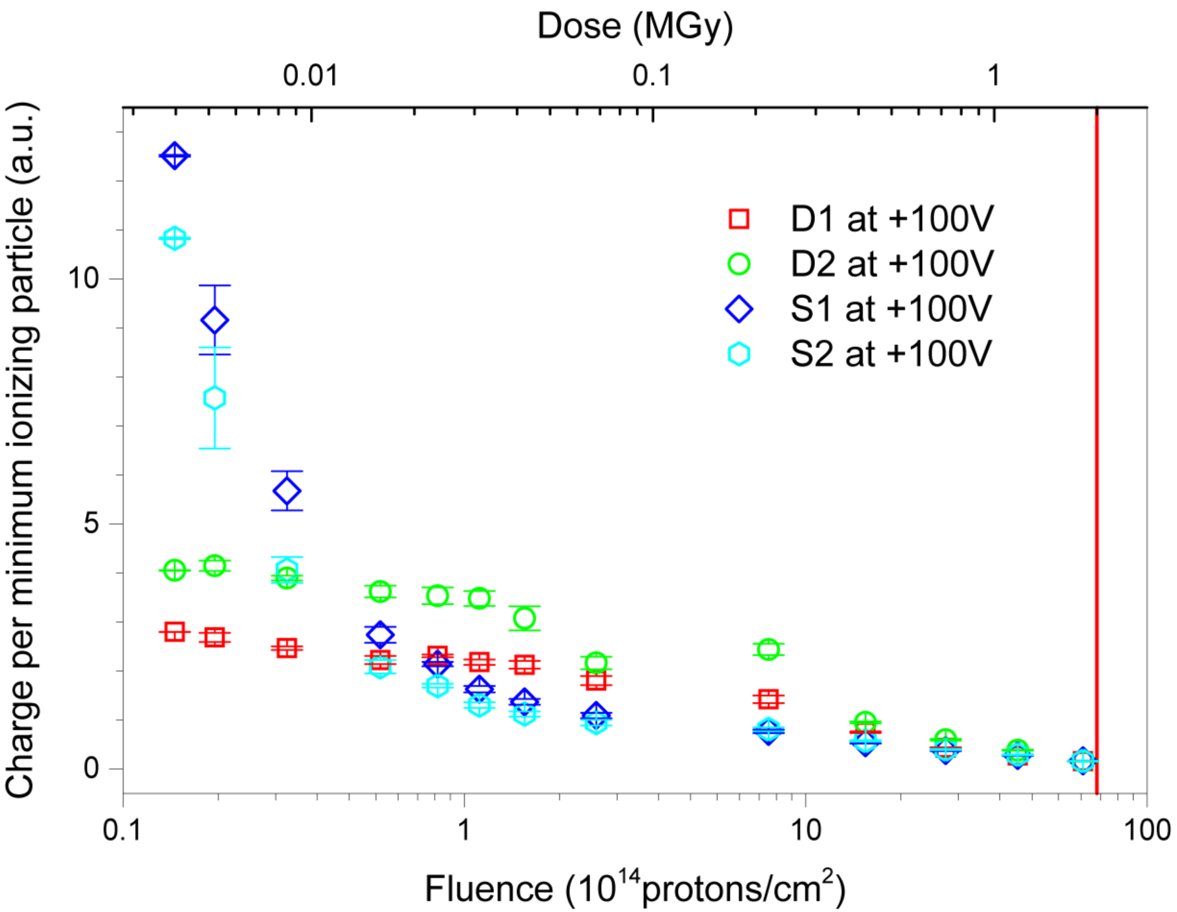

- All detectors biased by +100V (reverse bias for S1 and S2).

Results – charge vs. V_B

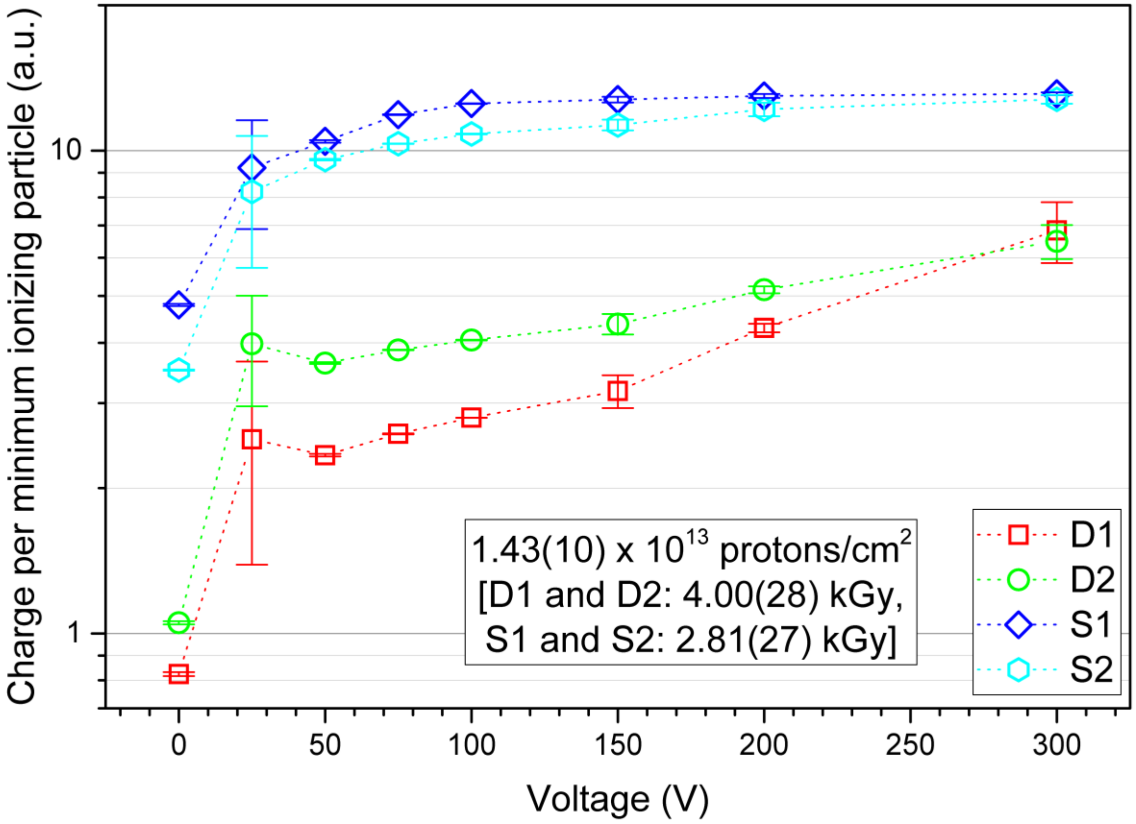

- D1 and D2 - 300µm and 500µm thick scCVD diamond detectors.
- S1 and S2 - 300µm thick p^+-n-n^+ Si detectors.

Results – charge vs. V_B

$$\frac{Q/MIPD_1(+150V)}{Q/MIPD_1(-150V)} = 54.1(33)\%$$

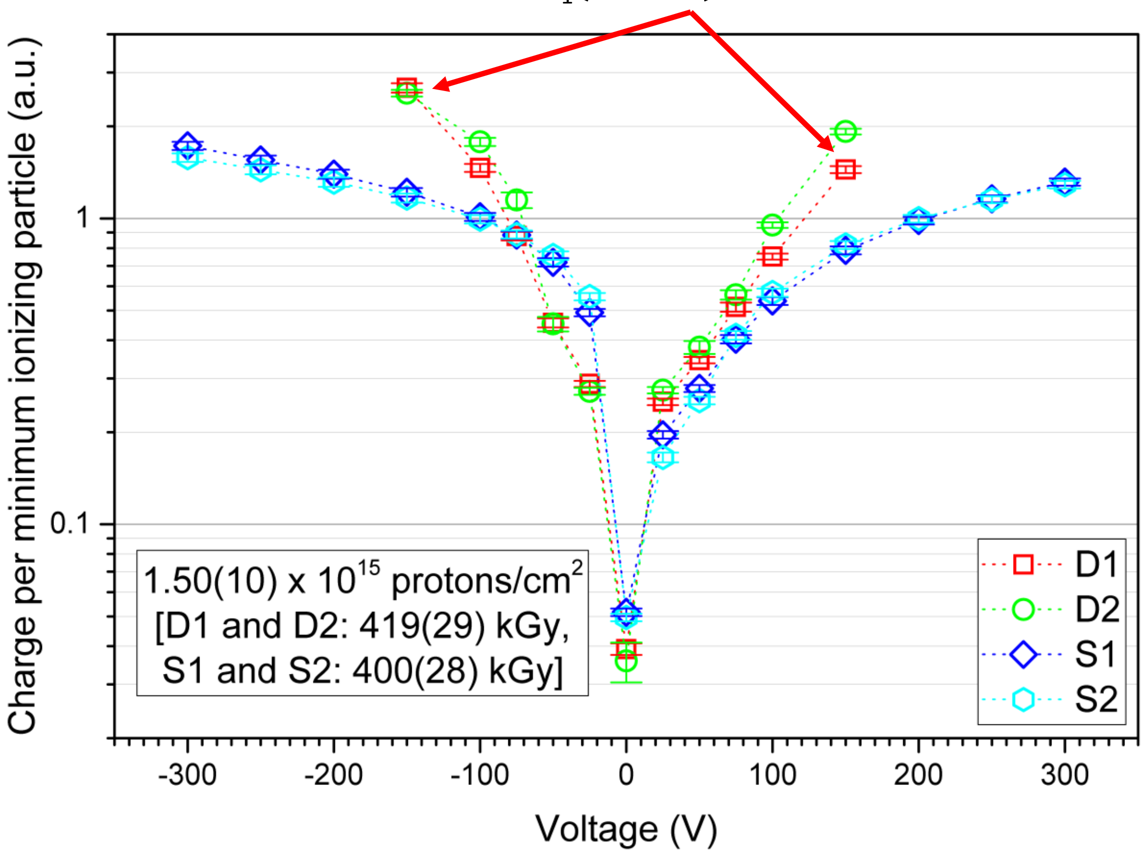

- An asymmetry of Q/MIP with respect to changing sign of V_B was observed when negative V_B was applied.

Results – charge vs. V_B

$$\frac{Q/MIPD_2(+150V)}{Q/MIPD_2(-150V)} = 75.0(36)\%$$

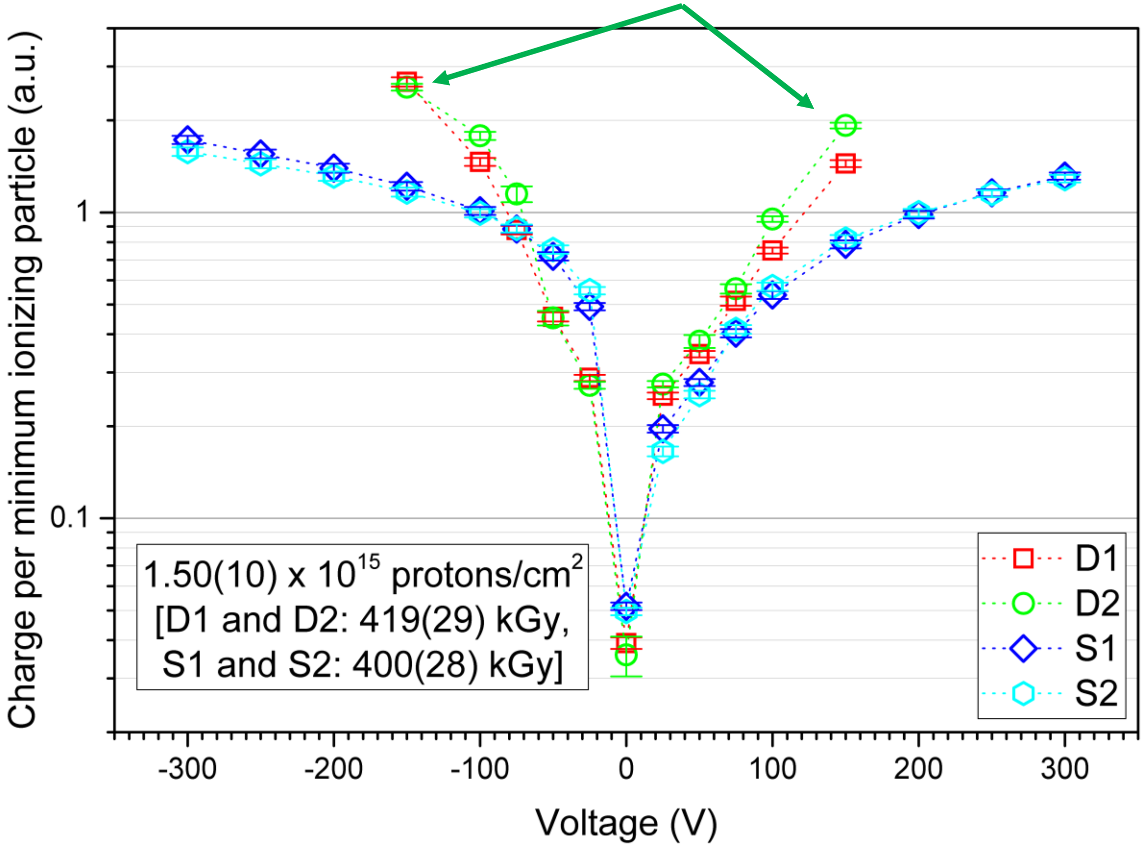

- An asymmetry of Q/MIP with respect to changing sign of V_B was observed when negative V_B was applied.

Results – charge vs. V_B

$$\frac{Q/MIPD_1(+300V)}{Q/MIPD_1(-300V)} = 79(23)\%$$

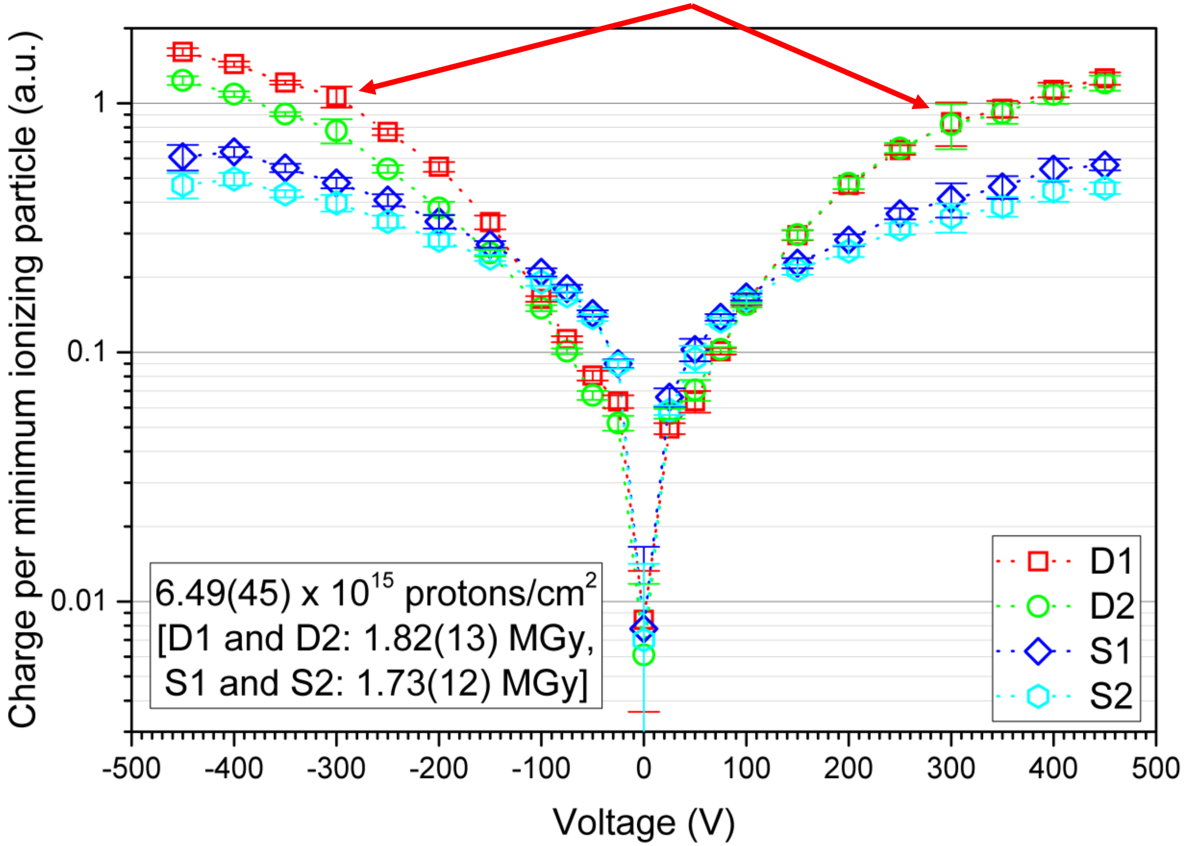

- At the end of the irradiation the asymmetry of Q/MIP with respect to changing sign of V_B was smaller.

Results – charge vs. V_B

$$\frac{Q/MIPD_2(+300V)}{Q/MIPD_2(-300V)} = 106(34)\%$$

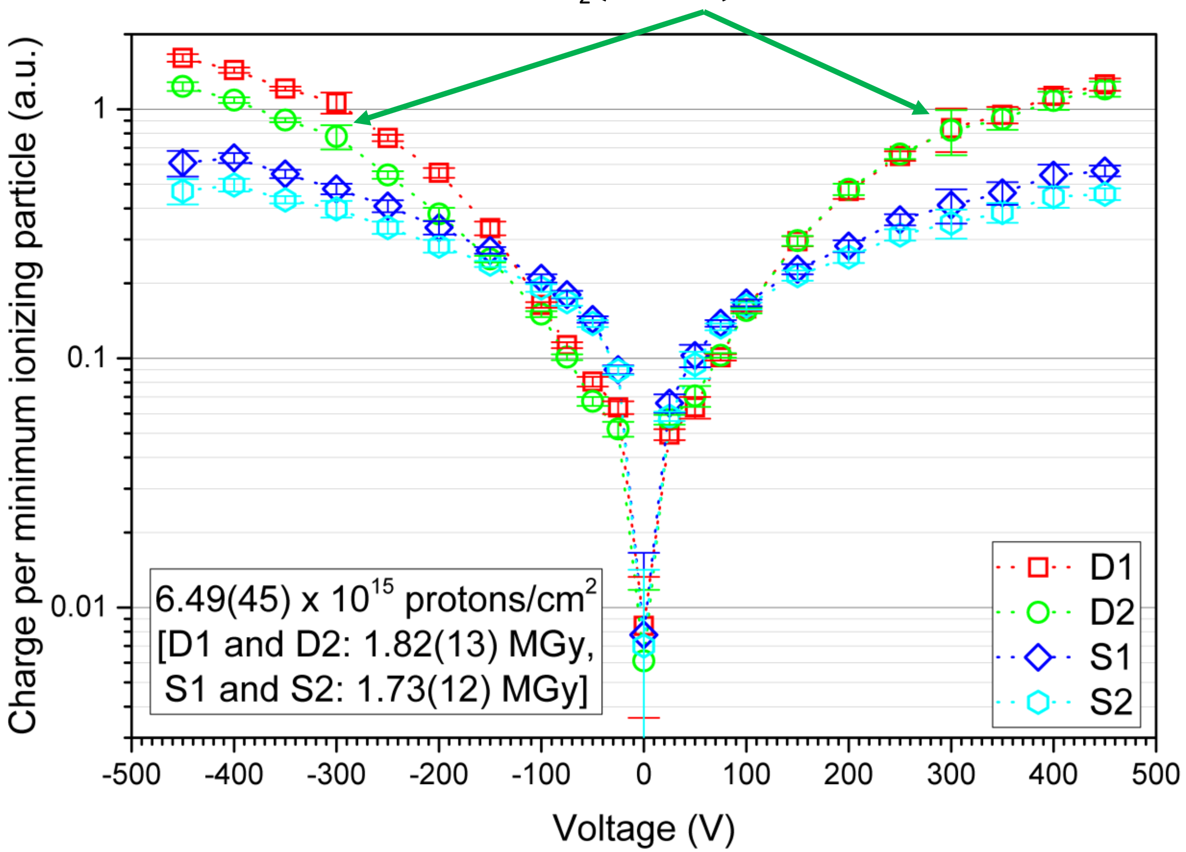

- At the end of the irradiation the asymmetry of Q/MIP with respect to changing sign of V_B was smaller.

Results – charge vs. V_B

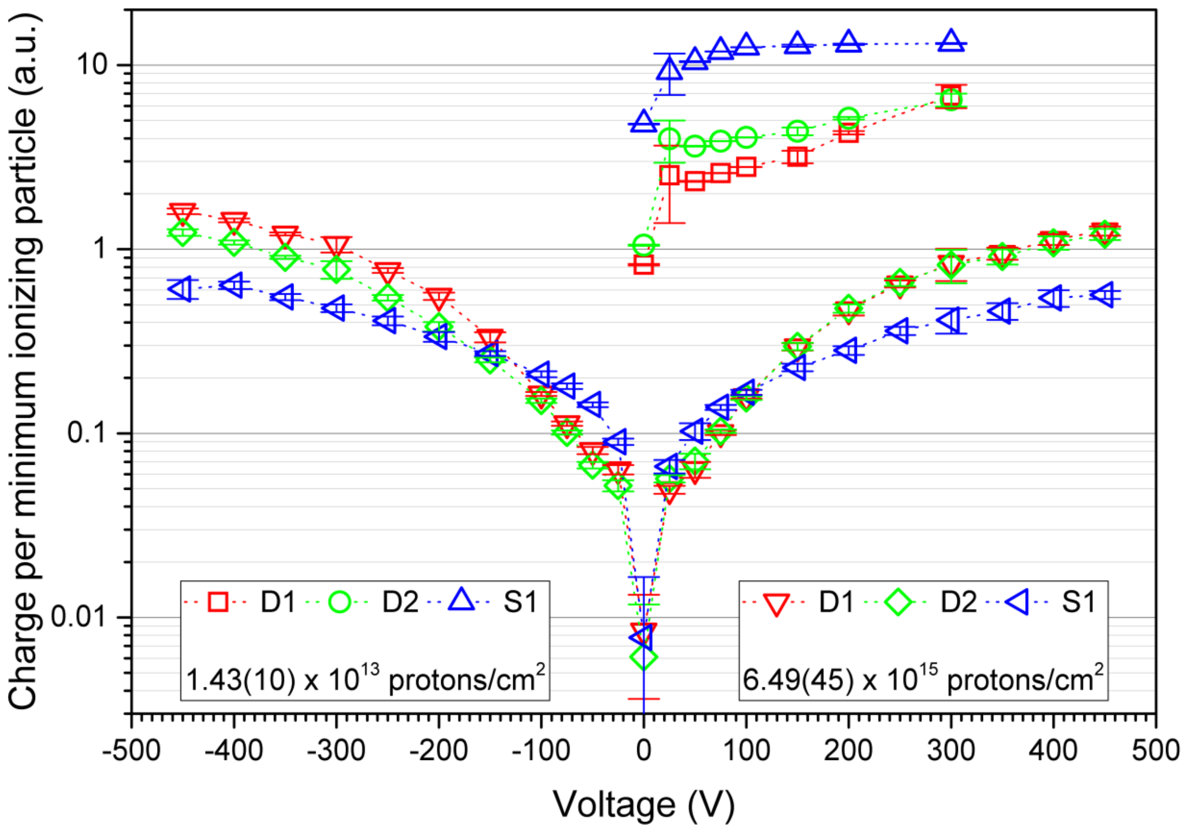

- During the irradiation:
- $Q/MIP_{D1}(+300V)$ decreased factor 8.1(28) and
- $Q/MIP_{D2}(+300V)$ decreased factor 7.9(23).
- As a comparison $Q/MIP_{S1}(+300V)$ decreased factor 31.8(52).

Results – charge vs. V_B

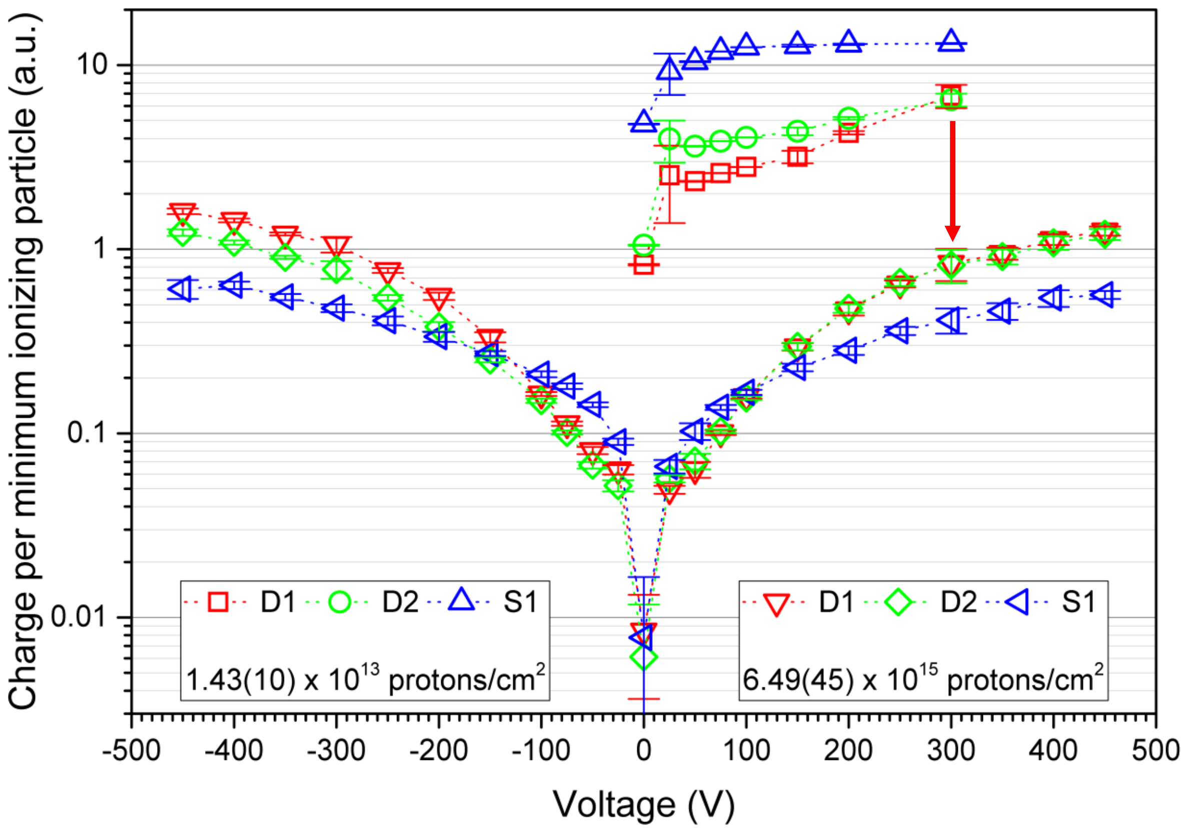

- During the irradiation:
- $Q/MIP_{D1}(+300V)$ decreased factor **8.1(28)** and
- $Q/MIP_{D2}(+300V)$ decreased factor 7.9(23).
- As a comparison $Q/MIP_{S1}(+300V)$ decreased factor 31.8(52).

Results – charge vs. V_B

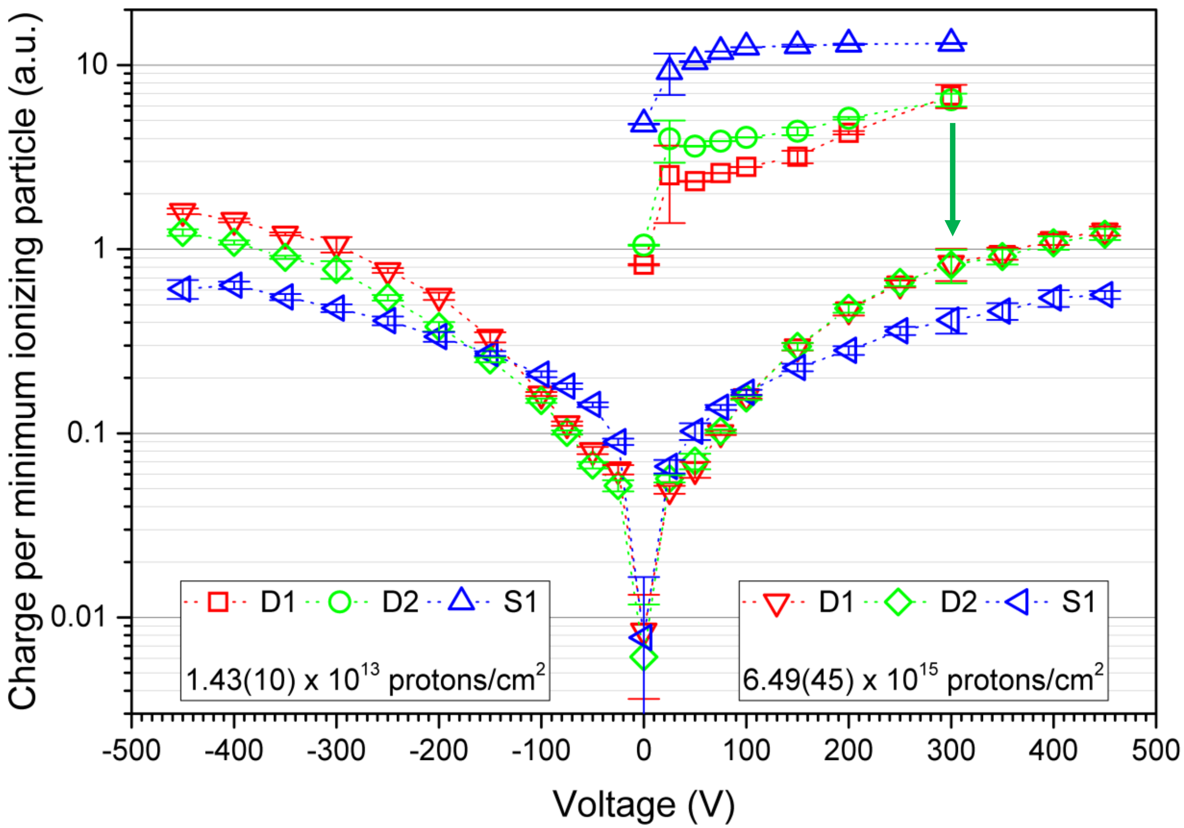

- During the irradiation:
- $Q/MIP_{D1}(+300V)$ decreased factor 8.1(28) and
- $Q/MIP_{D2}(+300V)$ decreased factor **7.9(23)**.
- As a comparison $Q/MIP_{S1}(+300V)$ decreased factor 31.8(52).

Results – charge vs. V_B

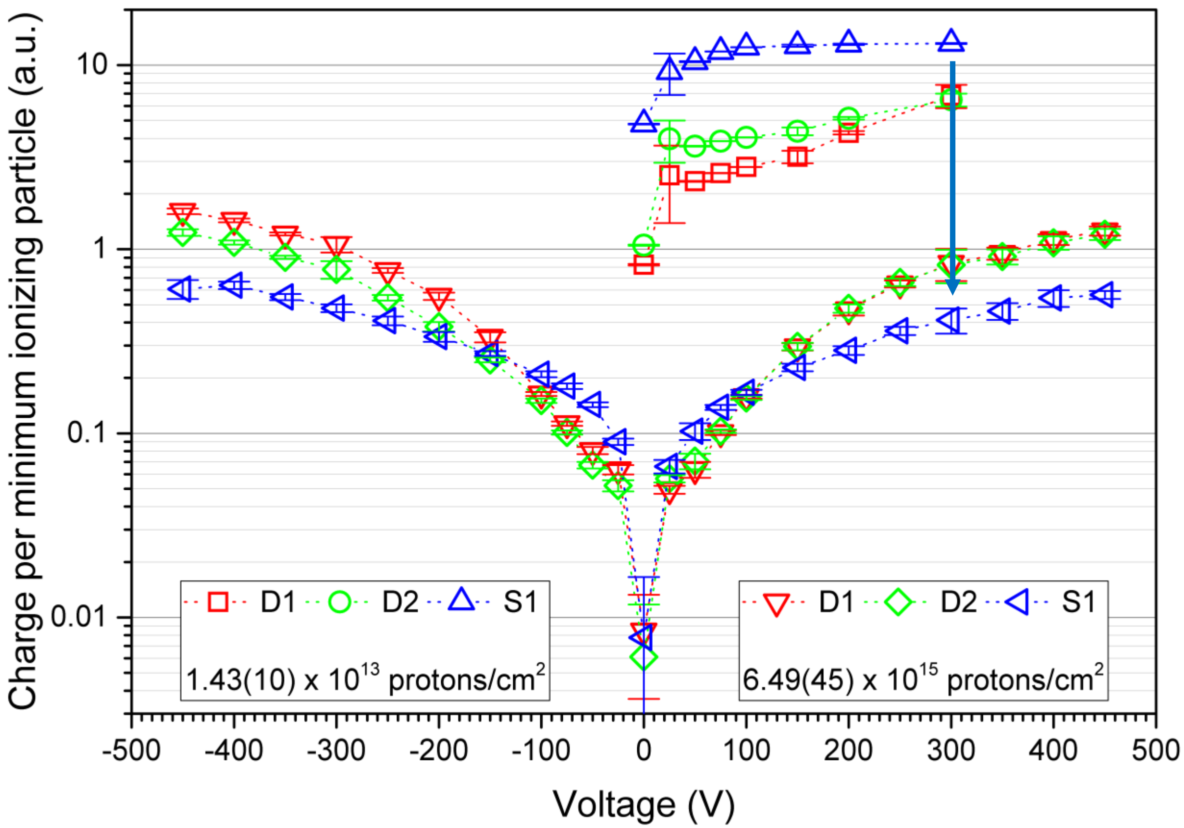

- During the irradiation:
- $Q/MIP_{D1}(+300V)$ decreased factor 8.1(28) and
- $Q/MIP_{D2}(+300V)$ decreased factor 7.9(23).
- As a comparison $Q/MIP_{S1}(+300V)$ decreased factor **31.8(52)**.

Tests of detectors in magnetic field

Requirements of Cryogenic BLMs

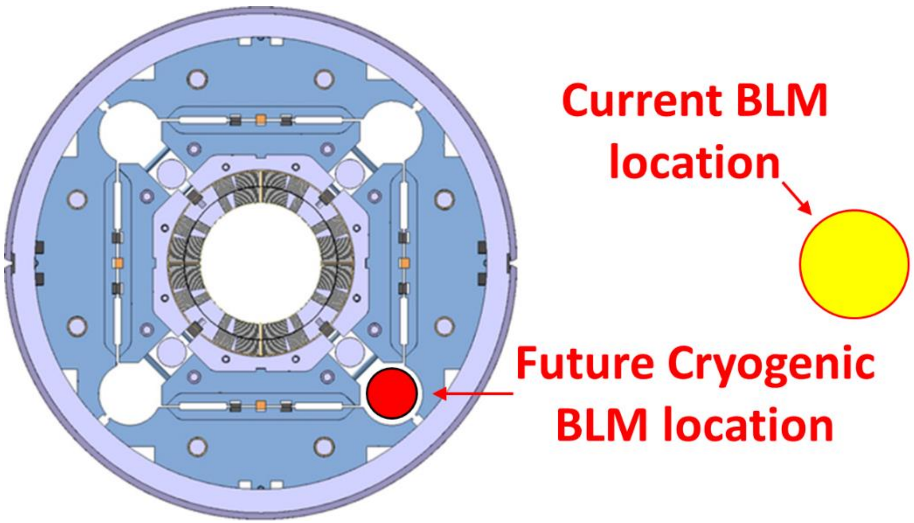

MQXF - courtesy of Paolo Ferracin

Mechanical requirements:

- total radiation dose of 2MGy,
- **low temperature of 1.9K,**
- 20 years, maintenance free operation,
- **resistance to magnetic field of 2T,**
- resistance to a pressure of 1.1 bar, and capability of withstanding a fast pressure rise up to 20bar in case of a magnet quench.

Electronic requirements:

- direct current readout,
- response linear between 0.1 and 10 mGy/s, and
- response time faster than 1 ms.

Diamonds in magnetic field

Transit time of electrons in RT (90deg inclination between electric and magnetic field)

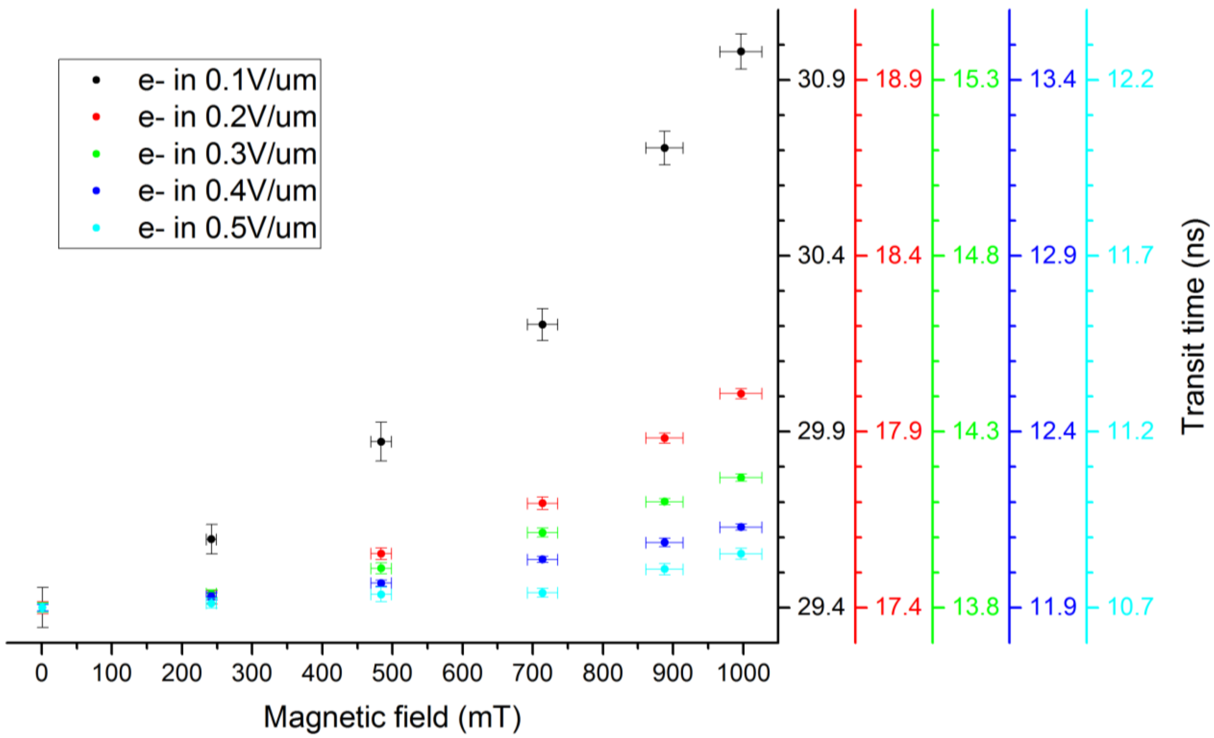

Diamonds in magnetic field

Transit time of holes in RT (90deg and 60deg inclination between electric and magnetic field)

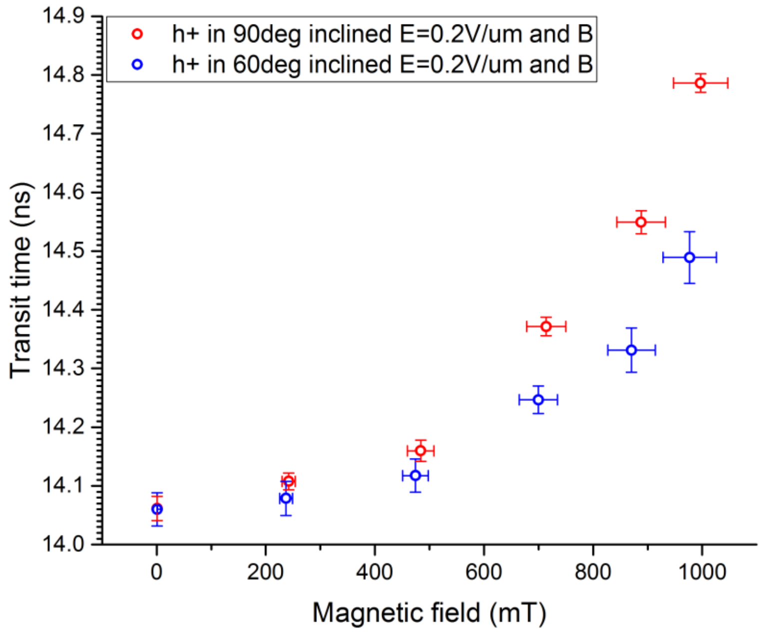

Diamonds in magnetic field

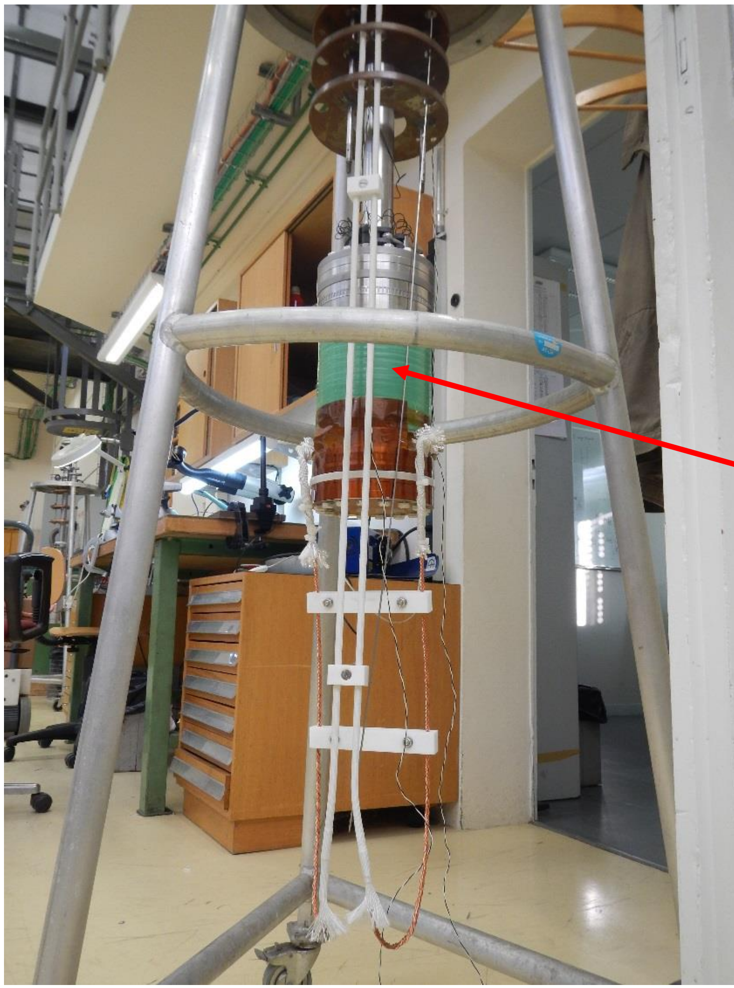

NbTi Coil

Thank you!